The effect of ionic correlations on radiative properties in the solar interior and terrestrial experiments

Menahem Krief,[1,*] Yair Kurzweil,[2] Alexander Feigel,[1] and Doron Gazit[1]

[1] *Racah Institute of Physics, The Hebrew University, 9190401 Jerusalem, Israel*
[2] *Physics Department, Nuclear Research Center-Negev, P.O. Box 9001, Beer-Sheva, Israel*

Intending to solve the decade old problem of solar opacity, we report substantial photoabsorption increase due to the effect of ion-ion correlation which was not heretofore considered. By performing detailed opacity calculations of the solar mixture, we find that taking into account the ionic structure results in a $\sim 10\%$ increase in the Rosseland opacity near the convection zone, which mimics the missing opacity profile required by helioseismology and neutrino observations. These results point out the correlation effect as a major source for the missing opacity and call for a detailed characterization of its uncertainties. We also report a $\sim 15\%$ increase in the Rosseland opacity for iron monochromatic opacity which was recently measured at the Sandia Z facility, where the temperature reached that prevailing in the convection zone while the density is 2.5 times lower. Finally, we propose a method to measure opacities at solar temperatures and densities that were never reached in the past via laboratory radiation flow experiments, by using plastic foams doped with permilles of dominant photon absorbers in the Sun. The method is an ideal candidate to experimentally study Rosseland opacities of the solar mixture.

arXiv:1611.09339v1 [astro-ph.SR] 28 Nov 2016

Radiation transport is of decisive importance in the modeling of a wide variety of high energy density plasmas as those encountered in stellar interior as well as in terrestrial laboratories, such as high power laser and Z-pinch facilities. The radiative opacity is a key quantity describing the coupling between radiation and matter which entails a sophisticated interplay of plasma and atomic physics.

Over the past decade, an outstanding open problem in solar physics has emerged, as solar photospheric abundances of metallic elements have been significantly revised downward [1–3]. Standard solar models cannot reproduce helioseismic measurements [4], such as the convection zone radius, the surface helium abundance and the sound speed profile, when using these revised abundances. This gave rise to the *solar composition problem*, motivating a rapid growth of research efforts in the field. The implications of this problem on astrophysical science are very large since stellar evolution theory, which is routinely used to interpret any star or stellar population, is calibrated on the Sun. Therefore, the knowledge about stars and galaxies is nowhere better than the current understanding of the Sun. In addition, the Sun has been extensively used for setting constraints on the properties of dark matter candidates [5].

Absorption by photoexcitation and photoionization of partially ionized metallic elements, which are only present as a few percent of the solar mixture, is the major source of opacity in the solar interior. Therefore, it is widely believed that in order for solar models to reproduce helioseismic observations, opacities of mid and high-Z elements, which are the most complicated to model theoretically from first principles and for which there is no experimental validation, should be revised upward to compensate for the decreased abundances. It has been shown [6–10] that a smooth increase of the solar opacity from the range of $\sim 5\%$ in the central regions to the range of $\sim 20\%$ near the convection zone boundary (CZB), reproduces helioseismic and neutrino flux observations, as demonstrated in Figure 1. Differences between first principles state of the art opacity models are too small to account for the *missing opacity*, giving rise to a *solar opacity problem*. Otherwise, assuming that opacities used currently in solar models are accurate, other parts of solar models must be altered, such as stellar atmosphere and spectroscopic models, mixing mechanisms and enhanced gravitational settling, or even non standard solar models incorporating rotation and magnetic fields, which are completely prohibitive with present day computational capabilities.

Recent laboratory measurements [11] of the monochromatic opacity of iron, a major photon absorber throughout the solar interior, were performed at the Sandia Z machine. The temperatures reached at these experiments match those found near the CZB, while the electron densities are about a factor of 2.5 lower. The measured spectra is larger than calculations of all available atomic models by $30\% - 400\%$. No satisfactory explanation for this discrepancy is yet known [12]. The observed upward revision of iron opacity supports the revised solar abundances and the missing opacity in solar physics, although at different plasma conditions than those found at the CZB.

Taking into account the complicated many-body interaction of a photon emitting/absorbing ion with the adjacent hot dense plasma in atomic calculation is a very important yet extremely challenging task in the field. These interactions give rise to important phenomena such as collisional line broadening [13–15] and ionization potential depression [16–20]. In addition, the plasma environment affects the local atomic central potential and the boundary conditions of atomic wavefunctions. In order

to calculate the latter effect properly, the ionic structure of the plasma, which is given by the ion-ion pair correlation function must be known. However, it is very challenging to calculate ionic correlations from first principles [21] and approximate models, which were never tested experimentally at stellar interior conditions, must be used. Opacity models frequently approximate the ionic structure in the framework of the rather crude Ion-Sphere (IS) model [22], in which the ionic structure is completely smeared out. The sensitivity of solar opacity calculations to the IS approximation was never analyzed in the context of the solar opacity problem.

In this work, plasma correlation effects are pointed out as a significant source of uncertainty in the calculation of solar opacities. The effects of plasma correlations beyond the IS model are studied by using the Ion-Correlation (IC) model by Rozsnyai [23, 24], which is a one component plasma model that includes a more realistic treatment of ionic structure. Detailed opacity calculations of the solar mixture throughout the solar radiative zone were preformed in order to compare the IS and IC models. We report a $\sim 10\%$ increase in the Rosseland opacity near the CZB and an opacity variation profile which assimilates the profile required by helioseismology and neutrino observations. These results highlight the plasma correlation effect as a major source for the missing opacity and call for further examination of the effect with more advanced plasma models [25]. The effect was also examined at the conditions of the recent Sandia experiment for which we find a $\sim 15\%$ increase in the Rosseland opacity. Finally, we highlight and analyze the possibility to measure Rosseland opacities at plasma conditions found within the solar interior, via terrestrial radiation flow experiments in high energy density laboratories, such as the National Ignition Facility (NIF) [26, 27], Laser-Megajoule [28], OMEGA [29] and Sandia Z-machine [11], by using plastic foams doped with permilles of dominant photon absorbers in the Sun, such as iron and oxygen. The range of temperature and electron density that can be achieved in such experiments, if performed at the NIF [26, 27], cover the conditions of the solar plasma at solar radii ranging from the CZB ($R/R_\odot = 0.72$) and deeper, up to $R/R_\odot \approx 0.55$, which were never achieved in laboratory experiments. In addition, ion-correlation effects can be directly observed in such experiments. This method is complementary to monochromatic experiments, which give much more detailed information on opacity spectra but cannot access the more important spectral range close to the Rosseland peak, are unable to reach the densities found near the CZB or the higher temperatures found in deeper regions, and which have a $20-30\%$ uncertainty in the measured electron density [30]. The radiation flow experiments, for which the latter drawbacks are irrelevant, are ideal candidates for an experimental study of Rosseland opacities of the solar plasma.

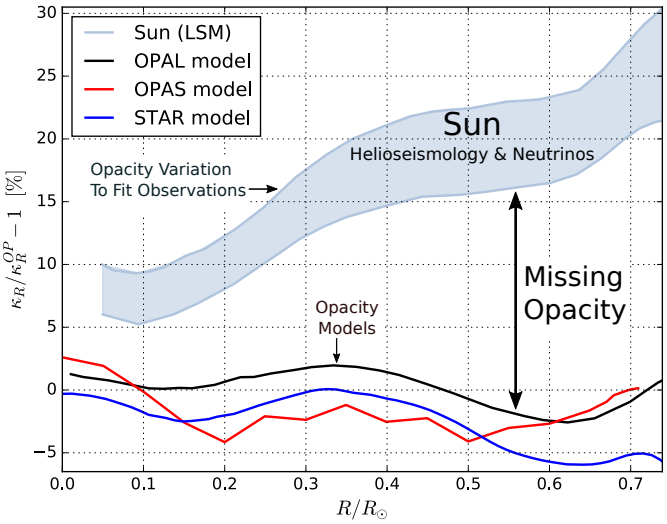

FIG. 1. **An illustration of the solar opacity problem**. The shaded area represents the range of required opacity variation across the solar interior, in order for helioseismic and neutrino observations to agree with solar model predictions. The solid curves represent relative differences in the Rosseland opacity $\kappa_R/\kappa_R^{OP} - 1$, between the OP opacity model [31] and the OPAL model [32] (in black), the OPAS model [33, 34] (in red) and the STAR model [15, 35] (in blue). The small discrepancies between opacity models cannot explain the missing opacity that is constrained by observations.

RESULTS

We have employed the opacity code STAR [15, 35, 36] to calculate the opacity of a 24-element solar mixture along a thermodynamic path obtained from a solar model implemented by Villante et al. [37] which is calibrated with the recent AGSS09 set of chemical abundances [2]. Bound-bound and bound-free atomic calculations are performed in the STA framework [38] and based on a fully relativistic quantum mechanical theory via the Dirac equation, while inverse bremsstrahlung is calculated via a screened hydrogenic approximation with a degeneracy correction [35]. Calculations were performed in the IS and IC approximation. In the IS model each ion is enclosed within a spherical volume whose radius r_{IS} is the Wigner-Seitz radius of the plasma. In addition, the ionic distribution vanishes inside the sphere while it is smeared out completely outside of it, so that the ion-ion pair correlation function $g(r)$ takes the form of a step function and due to overall charge neutrality the central potential vanishes outside the sphere. Such a model neglects the possibility for ionic charge to penetrate into the ion sphere and screen the central potential seen by atomic wavefunctions, as illustrated in Figure 2. On the other hand, the IC model [23, 24] includes a more realistic treatment of ionic structure which is solved self-consistently with the electronic structure and

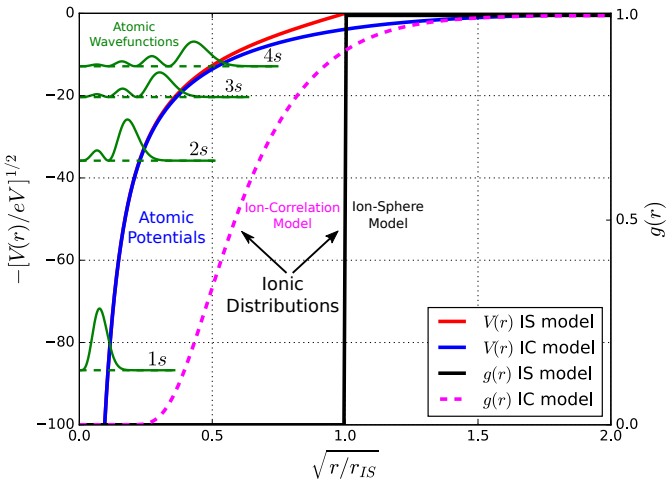

FIG. 2. **Models for the plasma surrounding an atom.** Shown are the central atomic potentials $V(r)$ (left axis) in the IS (red) and IC (blue) model, as well as the ion-ion pair correlation functions $g(r)$ (right axis) in the IS model (step function, in black) and IC model (magenta). The radial wavefunctions of the first four "s" orbitals are given in green (arbitrary units) where the vertical positions represent the orbital energies (on the left axis). The calculation was performed for iron near the convection zone boundary at $R/R_\odot = 0.72$, temperature $T = 180$eV and electron density $n_e = 8 \cdot 10^{22}\text{cm}^{-3}$.

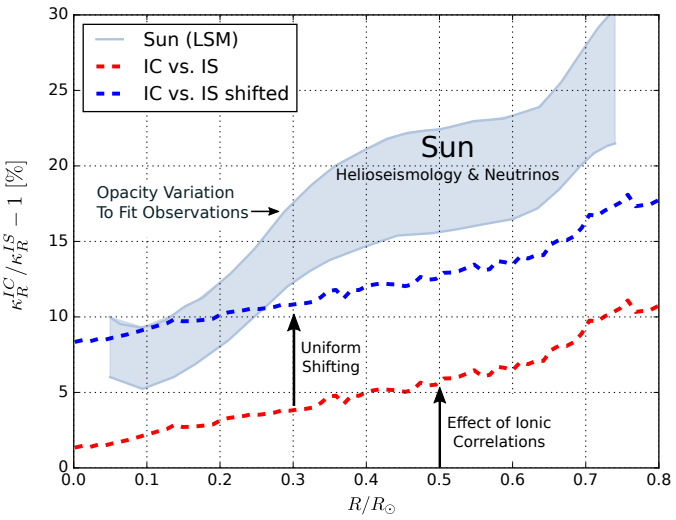

FIG. 3. **The effect of plasma correlations on the solar opacity**. Relative differences in the Rosseland opacity of the solar mixture throughout the solar interior, between Ion-Sphere and Ion-Correlation calculations (red line). The blue line is obtained by a constant 7% upward shift for a comparison of the shape of the resulting profile with that of the observational constraints, which is required for solar models to agree with the sound speed profile and convection zone radius, as observed by helioseismology (see text).

which screens the central potential. For strongly coupled plasmas (lower temperatures and higher densities) the ionic structure features the well known short range order, whereas for more weakly coupled plasmas, such as the solar mixture, it is smeared out while ions penetrate within the ion-sphere, as described in Figure 2. The longer range of the central potential in the IC model slightly widens the spatial range of bound orbitals. This causes an increase of the spatial overlap between bound and continuum states which in turn increase the photoionization cross section [23], enabling a non-negligible increase of the Rosseland opacity. In addition, the longer range of the potential slightly lowers the average ionization. We note that solar opacity calculations in the IC framework were performed in the past [24], using the older soler abundances [39].

The resulting variation, between IS and IC, in the Rosseland opacity of the solar mixture throughout the solar interior, is shown in Figure 3 (red line), together with the range of opacity variation required for solar models to agree with helioseismic and neutrino observations. A $\sim 10\%$ increase near the CZB, which is about half of the missing opacity, is obtained. In addition, we note that in order to reconcile only the observed and predicted sound speed profile and convection boundary radius, the opacity variation profile must only have a *shape* lying within the variation band, while its magnitude is only required to reconcile the observed neutrino fluxes and surface helium abundance [37]. Therefore, by a constant 7% upward shift of the resulting variation profile (blue line), it is evident that its shape is very similar to, and almost lies within the limits posed by the observational constraints for the sound speed profile and convection radius.

In Figure 4, the monochromatic opacities of iron calculated by STAR, at the conditions reached in the recent Sandia experiment [11] are shown. Similar results were obtained by using the CRSTA atomic code [40, 41]. The resulting Rosseland opacity in the IC model is larger by $\sim 15\%$ than in the IS model, due to a significant increase of the M-shell photoionization cross-section, which results from the larger overlap of the M-shell bound orbital with the continuum states in the IC calculation. We note that despite having a significant contribution to the Rosseland opacity, which peaks at a photon energy of $3.8k_BT$, the M-shell spectral range is currently not accessible in the $5.5 - 9.5k_BT$ spectral range reached in opacity experiments at the Sandia Z machine, which includes only the L-shell spectral range. We note that such required soft X-ray spectrometers are currently being developed [42]. It is seen from Figure 4 that the plasma correlation has a smaller effect on the more strongly bound L-shell orbitals, and therefore cannot explain the "higher than predicted" iron opacity [11], which is found in the L-shell spectral range. Hence, the correlation effect for iron cannot be measured currently in such a monochromatic experiment.

We now illustrate how Rosseland opacities at solar in-

terior conditions can be measured directly via radiation flow experiments [43–46] in high energy density facilities. In such experiments the Rosseland mean is inferred directly from the measured breakout time of an x-ray supersonic radiative wave crossing a foam, which is coupled to a high temperature thermal x-ray source, as illustrated in Figure 5a. Employing the NIF, a drive temperature of up to ~ 300eV can be reached [27], which covers the temperatures in the Sun ranging from the CZB ($R/R_\odot = 0.72$) and deeper, up to $R/R_\odot \approx 0.55$. By using low-Z foams, electron densities prevailing in the latter region of the Sun can also be achieved. Therefore, by doping the foam with permilles of dominant photon absorbers in the Sun, such as oxygen, magnesium and iron, the Rosseland opacity can be studied experimentally at solar interior conditions that were never achieved in the past. As an example, in Table I we list the properties of the CH, CH_2 and CH_4 plastic foams, doped with oxygen, neon, magnesium and iron with a number concentration of 0.25% each, at conditions found in the Sun at four different locations: $R/R_\odot = 0.72, 0.64, 0.58$ and 0.55. The foam densities corresponding to conditions at the solar interior are in the range of $0.3 - 1.3\text{g/cm}^3$. Plastic foams can be easily manufactured with various hydrogen to carbon ratios and with densities of up to $\sim 1\text{g/cm}^3$, which corresponds to $R/R_\odot = 0.58$, where the temperature is 280eV. The resulting ion-correlation effect is a non negligible $5 - 10\%$ in the Rosseland opacity, and therefore, can be validated experimentally [46]. The small amount of doping does not affect thermodynamic properties of the plasma such as the chemical potential, average ionization and electron density, while it significantly affects radiative properties. In Figure 5b we list the contributions of the different elements in the doped CH foam to its Rosseland opacity. It is evident that the majority of the opacity ($\gtrsim 60\%$) is due to the doped elements, with iron having the largest contribution ($\sim 40\%$), while the remaining $\lesssim 40\%$ is due to the carbon K-shell photoionization, which can can be significantly reduced by using lower Z foams. Since the opacity is highly dependent on the composition and amount of doping and also on the type of foam, by performing a series of experiments with varying amount of doping, composition and foams, the experimental errors can be reduced significantly. In addition, Rosseland opacity fractions of test elements can be easily measured by comparing the results of foams with and without the tested element. Finally we note that calibration and comparison of measurements with different foam setups is easily achieved by aligning the foams together, so that they would experience the same radiation drive.

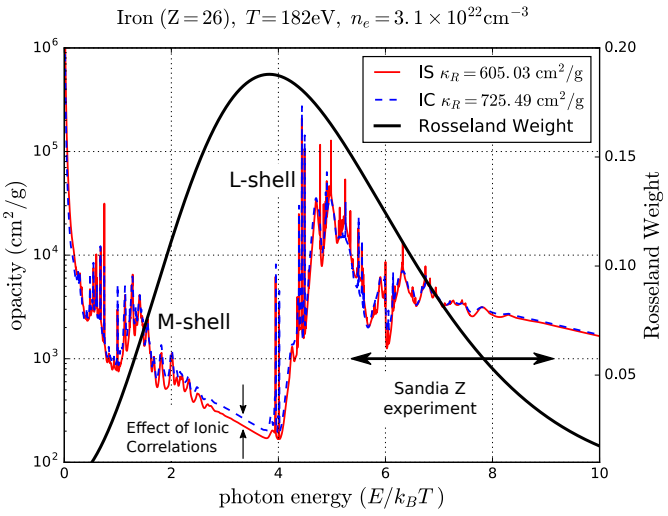

FIG. 4. **The effect of plasma correlations in the recent Sandia experiment.** The spectral opacity of iron (right axis) calculated by the IS (solid line, in red) and IC models (dashed line, in blue) at typical conditions reached by the recent Z-machine experiment [11] (temperature $T = 182$eV, free electron density $n_e = 3.1 \times 10^{22}\text{cm}^{-3}$). The Rosseland weight function (right axis) is shown in the solid black line. The experimentally accessible spectral range is indicated by a horizontal arrow. The Rosseland mean opacities are given in the legend.

SUMMARY

A significant increase to solar opacity calculations is required to solve the decade old disagreement between helioseismology and solar models. The small *discrepancy* in the solar mixture opacity between all existing atomic models is not a measure of the *accuracy* of these calculations, since similar physical models and approximations are used. An experimental validation of opacity calculations at stellar interior conditions, which has never been performed in the past, should aid significantly in understanding the source of the missing opacity.

In this work, the effect of ion-ion correlations which results from the extremely complex interaction between ions in a plasma, was pointed out as a source of uncertainty in the calculation of solar opacities. The effect was studied by using the Ion-Correlation model [23] which includes a more realistic treatment of ionic structure, that was not heretofore considered. We found a significant $\sim 10\%$ increase in the Rosseland opacity near the CZB and an opacity variation profile which assimilates the missing opacity required by helioseismology and neutrino observations. Hence, we conclude that correlation effects consist of an important ingredient of the missing opacity. This calls for a detailed examination of the effect with more advanced plasma models [21], since the IC calculations presented in this work were performed in the Debye-Huckel approximation. In a recent work [15] we

TABLE I. **Properties of doped plastic foams at terrestrial radiation flow experiments at solar interior conditions**. The average ionization $\bar{Z}$, required mass density ρ, Rosseland mean free path l_R and the relative difference in the Rosseland opacity between IC and IS, $\Delta\kappa_R$, are listed for doped CH, CH_2 and CH_4 (see text), with thermodynamic conditions (temperature T and electron density n_e), prevailing at the listed locations $R/R_\odot$ in the Sun. At $R/R_\odot = 0.58$ the required foam densities approach the maximal available density of $\sim 1\mathrm{g/cm}^3$ and at $R/R_\odot = 0.58$ the temperature of 300eV is the maximal temperature which is currently achievable in terrestrial laboratories.

		CH	CH_2	CH_4
$R/R_\odot = 0.72$	$\bar{Z}$	3.25	2.53	1.94
$T = 180$eV	$\rho\,[\mathrm{g/cm}^3]$	0.27	0.26	0.24
$n_e = 8\times10^{22}\mathrm{cm}^{-3}$	$l_R\,[\mathrm{mm}]$	0.13	0.12	0.12
	$\Delta\kappa_R$(IC/IS)	6.8%	7.2%	10.2%
$R/R_\odot = 0.64$	$\bar{Z}$	3.29	2.55	1.96
$T = 235$eV	$\rho\,[\mathrm{g/cm}^3]$	0.58	0.54	0.5
$n_e = 1.7\times10^{23}\mathrm{cm}^{-3}$	$l_R\,[\mathrm{mm}]$	0.12	0.11	0.1
	$\Delta\kappa_R$(IC/IS)	5.1%	6.6%	7.1%
$R/R_\odot = 0.58$	$\bar{Z}$	3.29	2.55	1.96
$T = 280$eV	$\rho\,[\mathrm{g/cm}^3]$	1.05	0.99	0.91
$n_e = 3.1\times10^{23}\mathrm{cm}^{-3}$	$l_R\,[\mathrm{mm}]$	0.1	0.09	0.08
	$\Delta\kappa_R$(IC/IS)	4.8%	4.9%	7.2%
$R/R_\odot = 0.55$	$\bar{Z}$	3.29	2.55	1.96
$T = 300$eV	$\rho\,[\mathrm{g/cm}^3]$	1.42	1.34	1.23
$n_e = 4.2\times10^{23}\mathrm{cm}^{-3}$	$l_R\,[\mathrm{mm}]$	0.09	0.08	0.07
	$\Delta\kappa_R$(IC/IS)	5.3%	5.6%	5.8%

have shown that uncertainties in line-broadening models, another plasma effect, also have a significant contribution to the missing opacity, and in fact, can account for all of the missing opacity, if the line-width uncertainty is of a factor of about ~ 100. The uncertainties in line broadening models which are used in opacity codes are unknown, as they were never tested experimentally at stellar interior conditions. However, a factor of ~ 100 seems to be too large, since differences between line-width models are typically factors of $2-15$. The ion-ion correlations effect which was studied in this work, may compensate for the remaining missing opacity with such moderate factors. A detailed analysis which includes a sound theoretical or experimental quantification of the uncertainties due the various plasma effects, which depends solely on the temperature and free electron density, is called for.

We also examined the correlation effect for iron conditions reached at the recent Sandia experiment [11] and found a $\sim 15\%$ increase in the Rosseland opacity, which is mainly due to an increase of the M-shell photoionization cross section, which cannot be accessed experimentally with current spectrometers.

Finally, we have analyzed the possibility to measure Rosseland opacities via radiation flow experiments in high energy density facilities, by using plastic foams doped with permilles of dominant photon absorbers in the Sun, and shown that it is possible to cover the temperatures and densities of the solar plasma at solar radii ranging from the CZB ($R/R_\odot = 0.72$) and deeper, up to $R/R_\odot \approx 0.58$ which were never achieved in laboratory experiments. We have also shown that ion-correlation effects can be observed directly in such experiments. The method is complementary and advantageous to monochromatic Z experiments, which give detailed information on opacity spectra, but have several drawbacks: (i) the inability to access the more important spectral range closer to the Rosseland peak, (ii) only electron densities smaller by a factor of ~ 2.5 than those found near the CZB can be reached due to hydrodynamic expansion of the sample [30] (iii) the measured electron densities are uncertain by $20-30\%$ [47] since they are inferred from crude line broadening models for Mg K-shell lines and (iv) higher temperatures found in deeper regions in the Sun cannot be reached. These disadvantages are overcome in radiation flow experiments for which: (i) Only Rosseland opacities are measured, (ii) plastic foams can be manufactured at densities corresponding to the solar plasma in the range $R/R_\odot = 0.72-0.58$ and there is no hydrodynamic expansion of the foam since the radiative heat wave is supersonic, (iii) the foam density, which is known to a high precision, determines the electron density and (iv) temperatures of up to 300eV can be reached [27]. Hence, radiation flow experiments are an ideal method for an experimental study of Rosseland opacities of the solar plasma.

The authors thank Aldo Serenelli and Francesco Villante for providing solar data. We also thank Joseph Oreg for useful suggestions and comments.

* e-mail address: menahem.krief@mail.huji.ac.il

[1] Martin Asplund, Nicolas Grevesse, and A Jacques Sauval, "The solar chemical composition," in *Cosmic abundances as records of stellar evolution and nucleosynthesis*, Vol. 336 (2005) p. 25.
[2] Martin Asplund, Nicolas Grevesse, A Jacques Sauval, and Pat Scott, "The chemical composition of the sun," arXiv preprint arXiv:0909.0948 (2009).
[3] Grevesse, Nicolas, Scott, Pat, Asplund, Martin, and Jacques Sauval, A., "The elemental composition of the sun," A&A **573**, A27 (2015).
[4] Sarbani Basu and HM Antia, "Constraining solar abundances using helioseismology," The Astrophysical Journal Letters **606**, L85 (2004).
[5] Helmut Schlattl, Achim Weiss, and Georg Raffelt, "Helioseismological constraint on solar axion emission," Astroparticle Physics **10**, 353–359 (1999).
[6] Jørgen Christensen-Dalsgaard, Maria Pia Di Mauro,

Günter Houdek, and Frank Pijpers, "On the opacity change required to compensate for the revised solar composition," Astronomy & Astrophysics **494**, 205–208 (2009).
[7] Aldo M Serenelli, Sarbani Basu, Jason W Ferguson, and Martin Asplund, "New solar composition: the problem with solar models revisited," The Astrophysical Journal Letters **705**, L123 (2009).
[8] FL Villante, "Constraints on the opacity profile of the sun from helioseismic observables and solar neutrino flux measurements," The Astrophysical Journal **724**, 98 (2010).
[9] FL Villante and B Ricci, "Linear solar models," The Astrophysical Journal **714**, 944 (2010).
[10] FL Villante and AM Serenelli, "A quantitative analysis of the solar composition problem," Physics Procedia **61**, 366–375 (2015).
[11] JE Bailey, T Nagayama, GP Loisel, GA Rochau, C Blancard, J Colgan, Ph Cosse, G Faussurier, CJ Fontes, F Gilleron, *et al.*, "A higher-than-predicted measurement of iron opacity at solar interior temperatures," Nature **517**, 56–59 (2015).
[12] Sultana N Nahar and Anil K Pradhan, "Large enhancement in high-energy photoionization of fe xvii and missing continuum plasma opacity," Physical Review Letters **116**, 235003 (2016).
[13] Milan S Dimitrijevic and Nikola Konjevic, "Simple estimates for stark broadening of ion lines in stellar plasmas," Astronomy and Astrophysics **172**, 345–349 (1987).
[14] Hans R Griem, *Principles of plasma spectroscopy*, Vol. 2 (Cambridge University Press, 2005).
[15] M. Krief, A. Feigel, and D. Gazit, "Line broadening and the solar opacity problem," The Astrophysical Journal **824**, 98 (2016).
[16] O Ciricosta, SM Vinko, H-K Chung, B-I Cho, CRD Brown, T Burian, J Chalupskỳ, K Engelhorn, RW Falcone, C Graves, *et al.*, "Direct measurements of the ionization potential depression in a dense plasma," Physical review letters **109**, 065002 (2012).
[17] DJ Hoarty, P Allan, SF James, CRD Brown, LMR Hobbs, MP Hill, JWO Harris, J Morton, MG Brookes, R Shepherd, *et al.*, "Observations of the effect of ionization-potential depression in hot dense plasma," Physical review letters **110**, 265003 (2013).
[18] SM Vinko, O Ciricosta, and JS Wark, "Density functional theory calculations of continuum lowering in strongly coupled plasmas," Nature communications **5** (2014).
[19] LB Fletcher, AL Kritcher, A Pak, T Ma, T Döppner, C Fortmann, L Divol, OS Jones, OL Landen, HA Scott, *et al.*, "Observations of continuum depression in warm dense matter with x-ray thomson scattering," Physical review letters **112**, 145004 (2014).
[20] O Ciricosta, SM Vinko, B Barbrel, DS Rackstraw, TR Preston, T Burian, J Chalupskỳ, BI Cho, H-K Chung, GL Dakovski, *et al.*, "Measurements of continuum lowering in solid-density plasmas created from elements and compounds," Nature communications **7** (2016).
[21] Jérôme Daligault, Scott D Baalrud, Charles E Starrett, Didier Saumon, and Travis Sjostrom, "Ionic transport coefficients of dense plasmas without molecular dynamics," Physical review letters **116**, 075002 (2016).
[22] David A Liberman, "Self-consistent field model for condensed matter," Physical Review B **20**, 4981 (1979).
[23] Balazs F Rozsnyai, "Photoabsorption in hot plasmas based on the ion-sphere and ion-correlation models," Physical Review A **43**, 3035 (1991).
[24] Balazs F Rozsnyai, "Solar opacities based on the ion-sphere and ion-correlation models," The Astrophysical Journal **393**, 409–413 (1992).
[25] CE Starrett, D Saumon, J Daligault, and S Hamel, "Integral equation model for warm and hot dense mixtures," Physical Review E **90**, 033110 (2014).
[26] John D Lindl, Peter Amendt, Richard L Berger, S Gail Glendinning, Siegfried H Glenzer, Steven W Haan, Robert L Kauffman, Otto L Landen, and Laurence J Suter, "The physics basis for ignition using indirect-drive targets on the national ignition facility," Physics of Plasmas (1994-present) **11**, 339–491 (2004).
[27] Alastair S Moore, Thomas M Guymer, John Morton, Benjamin Williams, John L Kline, Nicholas Bazin, Christopher Bentley, Shelly Allan, Katie Brent, Andrew J Comley, *et al.*, "Characterization of supersonic radiation diffusion waves," Journal of Quantitative Spectroscopy and Radiative Transfer **159**, 19–28 (2015).
[28] Noël Fleurot, Claude Cavailler, and JL Bourgade, "The laser megajoule (lmj) project dedicated to inertial confinement fusion: Development and construction status," Fusion Engineering and Design **74**, 147–154 (2005).
[29] C Decker, RE Turner, OL Landen, LJ Suter, P Amendt, HN Kornblum, BA Hammel, TJ Murphy, J Wallace, ND Delamater, *et al.*, "Hohlraum radiation drive measurements on the omega laser," Physical review letters **79**, 1491 (1997).
[30] T Nagayama, JE Bailey, G Loisel, GA Rochau, JJ MacFarlane, and I Golovkin, "Calibrated simulations of z opacity experiments that reproduce the experimentally measured plasma conditions," Physical Review E **93**, 023202 (2016).
[31] MJ Seaton, Yu Yan, D Mihalas, and Anil K Pradhan, "Opacities for stellar envelopes," Monthly Notices of the Royal Astronomical Society **266**, 805–828 (1994).
[32] Carlos A Iglesias and Forrest J Rogers, "Updated OPAL opacities," The Astrophysical Journal **464**, 943 (1996).
[33] Christophe Blancard, Philippe Cossé, and Gérald Faussurier, "Solar Mixture Opacity Calculations Using Detailed Configuration and Level Accounting Treatments," The Astrophysical Journal **745**, 10 (2012).
[34] Guillaume Mondet, Christophe Blancard, Philippe Cossé, and Gérald Faussurier, "Opacity calculations for solar mixtures," The Astrophysical Journal Supplement Series **220**, 2 (2015).
[35] M Krief, A Feigel, and D Gazit, "Solar opacity calculations using the super-transition-array method," The Astrophysical Journal **821**, 45 (2016).
[36] Menahem Krief and Alexander Feigel, "The effect of first order superconfiguration energies on the opacity of hot dense matter," High Energy Density Physics **15**, 59–66 (2015).
[37] Francesco L Villante, Aldo M Serenelli, Franck Delahaye, and Marc H Pinsonneault, "The chemical composition of the sun from helioseismic and solar neutrino data," The Astrophysical Journal **787**, 13 (2014).
[38] A Bar-Shalom, J Oreg, WH Goldstein, D Shvarts, and A Zigler, "Super-transition-arrays: A model for the spectral analysis of hot, dense plasma," Physical Review A **40**, 3183 (1989).

[39] N Grevesse and A Noels, "Cosmic abundances of the elements." in *Origin and Evolution of the Elements*, Vol. 1 (1993) pp. 15–25.

[40] G Hazak and Y Kurzweil, "A Configurationally-Resolved-Super-Transition-Arrays method for calculation of the spectral absorption coefficient in hot plasmas," High Energy Density Physics **8**, 290–297 (2012).

[41] Y Kurzweil and G Hazak, "Inclusion of UTA widths in the Configurationally Resolved Super-Transition-Arrays (CRSTA) method," High Energy Density Physics **9**, 548–552 (2013).

[42] J Benstead, AS Moore, MF Ahmed, J Morton, TM Guymer, R Soufli, T Pardini, RL Hibbard, CG Bailey, PM Bell, *et al.*, "A new streaked soft x-ray imager for the national ignition facility," Review of Scientific Instruments **87**, 055110 (2016).

[43] TJ Orzechowski, MD Rosen, HN Kornblum, JL Porter, LJ Suter, AR Thiessen, and RJ Wallace, "The rosseland mean opacity of a mixture of gold and gadolinium at high temperatures," Physical review letters **77**, 3545 (1996).

[44] CA Back, JD Bauer, OL Landen, RE Turner, BF Lasinski, JH Hammer, MD Rosen, LJ Suter, and WH Hsing, "Detailed measurements of a diffusive supersonic wave in a radiatively heated foam," Physical review letters **84**, 274 (2000).

[45] CA Back, JD Bauer, JH Hammer, BF Lasinski, RE Turner, PW Rambo, OL Landen, LJ Suter, MD Rosen, and WW Hsing, "Diffusive, supersonic x-ray transport in radiatively heated foam cylinders," Physics of Plasmas (1994-present) **7**, 2126–2134 (2000).

[46] CL Fryer, E Dodd, W Even, CJ Fontes, C Greeff, A Hungerford, J Kline, K Mussack, I Tregillis, JB Workman, *et al.*, "Uncertainties in radiation flow experiments," High Energy Density Physics **18**, 45–54 (2016).

[47] T Nagayama, JE Bailey, G Loisel, GA Rochau, SB Hansen, C Blancard, P Cosse, G Faussurier, F Gilleron, J-C Pain, *et al.*, "Model uncertainties of local-thermodynamic-equilibrium k-shell spectroscopy," High Energy Density Physics (2016).

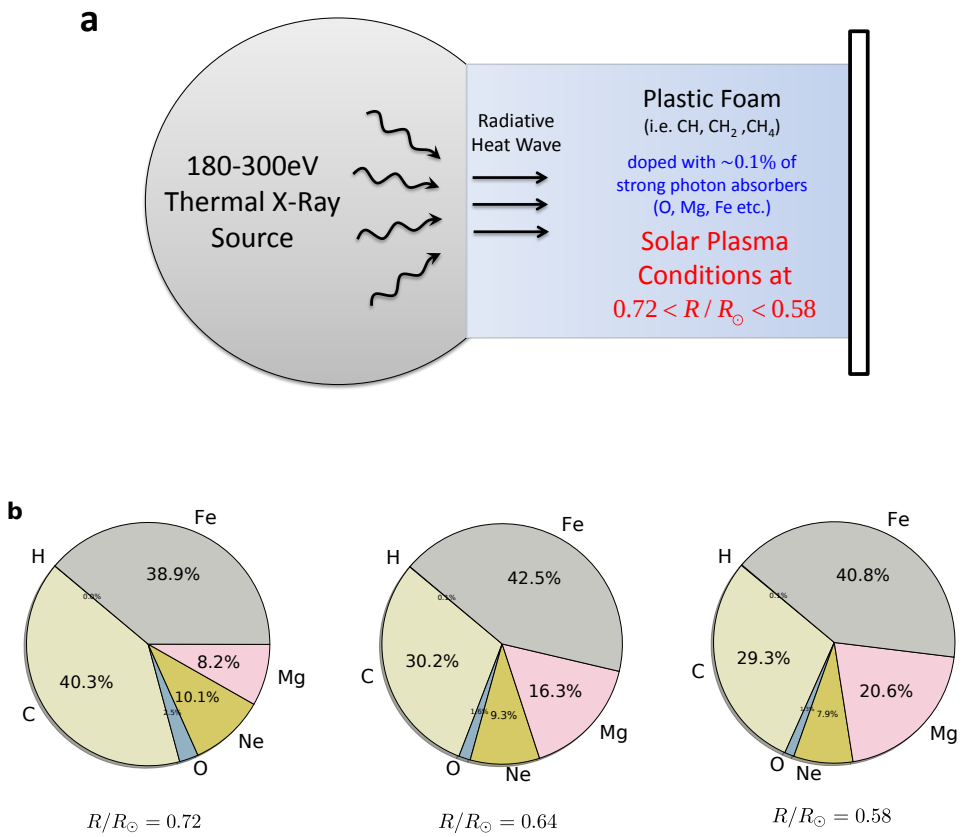

FIG. 5. **Illustration of a terrestrial radiation flow experiment to simulate the hot dense solar plasma.** (**a**) The side view shows a thermal x-ray source, coupled to a plastic foam such as CH, CH_2 and CH_4. An x-ray drive with a typical temperature of $180-300$eV, which can be produced at high energy density facilities, generates a supersonic radiative heat wave through the foam. The Rosseland opacity of the foam is inferred directly from the measured breakout time of the radiative wave through the foam. By doping the foam with permilles of strong photon absorbers in the Sun, such as oxygen and iron, the Rosseland opacity of a mixture with plasma parameters identical to those prevailing in the solar interior can be studied experimentally. (**b**) The charts represent Rosseland opacity contributions of the CH foam due to hydrogen, carbon and the doped elements, O, Ne, Mg, and Fe (with doping of 0.25% each, see text) at three thermodynamic conditions representing different positions in the Sun: $R/R_\odot = 0.72$ (left panel, $T = 180$eV, $n_e = 8\times10^{22}\mathrm{cm}^{-3}$), $R/R_\odot = 0.64$ (middle panel, $T = 235$eV, $n_e = 1.7\times10^{23}\mathrm{cm}^{-3}$) and $R/R_\odot = 0.58$ (right panel, $T = 280$eV, $n_e = 3.1\times10^{23}\mathrm{cm}^{-3}$). Additional properties of the CH foam under these conditions are listed in Table I.